colloid.[4] Both effects, the adsorption bleaching and the barrier to the addition of a second electron, may result either from band filling by the excess electron or from the local electric field created by the presence of the electron, even when it is localized.

Following the fast process, a second slower electron-transfer process is observed accompanied by a second proton-transfer process. The final conductivities from the pulse radiolysis are in good agreement with the observed $G(Pb(II))$ values from the steady-state experiments, both indicating some adsorption of lead(II) species onto the particle surface.

Acknowledgment. Work at Argonne National Laboratory is performed under the auspices of the Office of Basic Energy Sciences, Division of Chemical Science, US-DOE, under Contract No. W-31-109-ENG-38. The dedicated Linac operation by D. Ficht and G. Cox is much appreciated. P.M. acknowledges the receipt of a Commonwealth Postgraduate Research Award. Electrochemically prepared PbO_2 was a gift from M. Horne, CSIRO, Division of Mineral Products.

Registry No. ZV^-, 113111-40-3; PbO_2, 1309-60-0.

Surface Catalytic Sites Prepared from $[HRe(CO)_5]$ and $[H_3Re_3(CO)_{12}]$: Mononuclear, Trinuclear, and Metallic Rhenium Catalysts Supported on MgO

P. S. Kirlin,[†] F. B. M. van Zon,[‡] D. C. Koningsberger,[‡] and B. C. Gates*,[†]

Center for Catalytic Science and Technology, Department of Chemical Engineering, University of Delaware, Newark, Delaware 19716, and Laboratory of Inorganic Chemistry and Catalysis, Eindhoven University of Technology, P.O. Box 513, 5600 MB Eindhoven, The Netherlands *(Received: January 23, 1990; In Final Form: June 6, 1990)*

MgO-supported catalysts were prepared from $[HRe(CO)_5]$ and $[H_3Re_3(CO)_{12}]$ and characterized by extraction of surface organometallics, infrared and ultraviolet/visible spectroscopy, and extended X-ray absorption fine structure (EXAFS) spectroscopy. The EXAFS analysis and other data show that $[H_3Re_3(CO)_{12}]$ was initially deprotonated on the MgO surface, giving a surface-bound anion with a structure comparable to that of the salt $[Ph_4As][H_2Re_3(CO)_{12}]$ and having a Re–Mg distance of 2.39 Å. Heating of the supported cluster anion in helium to 225 °C led to oxidation and breakup of the cluster framework, giving a mononuclear complex formulated as $[Re(CO)_3\{OMg\}_3]$ (where the braces refer to groups terminating the bulk oxide). The distances characterizing the bonding of the Re to the support are Re–O = 2.15 Å and Re–Mg = 2.80 Å. A Re–Re distance of 3.94 Å was observed, consistent with the decomposition of the cluster on the support to form ensembles consisting of three of the Re subcarbonyls, for which a structural model is presented. Treatment of this sample in hydrogen at 350 °C gave a Re species with oxygen neighbors at average distances of 1.94 and 2.45 Å. Heating of this sample to 500 °C in hydrogen led to reduction and conversion of most of the Re into metal crystallites. The several samples were tested as catalysts, as described in a companion paper.

Introduction

Understanding of the catalytic activities of transition metals for rupture of C–H and C–C bonds in alkanes, important in the conversion of petroleum and petrochemicals, has been a goal of researchers for decades.[1,2] Progress has been hampered by the seeming impossibility of determining the contribution of a single, isolated active site of a structurally nonuniform metal catalyst[3,4] and by the lack of molecular models that catalyze the intermolecular rupture of C–C bonds (hydrogenolysis).[5,6] The results of kinetics investigations with supported metal catalysts indicate that the C–C bond breaking in alkane hydrogenolysis is preceded by multiple dehydrogenation steps and that the active site is comprised of more than one surface metal atom.[2,3,7] Multiple dehydrogenation (C–H insertion) of cycloalkanes has been observed with soluble mononuclear Re complexes; the extent of dehydrogenation increases with decreasing ring size from eight to five carbon atoms.[8,9] These results suggest that an ensemble of metal atoms with labile ligands may catalyze dehydrogenation of alkanes through C–H insertion, leading to the rupture of the C–C bond on adjoining metal centers.[10]

The goal of the present research was to prepare metal oxide supported Re catalysts consisting of ensembles of varying nuclearities (numbers of Re atoms) and to determine how the nuclearity influences the catalytic properties for activation of the C–C bond. A mononuclear precursor, $[HRe(CO)_5]$, was used to prepare surface structures designed to incorporate isolated surface-bound Re carbonyl complexes. A trinuclear precursor, $[H_3Re_3(CO)_{12}]$, was used to prepare ensembles consisting of three such complexes. The surface chemistry has been characterized by extraction of surface anions and infrared and other spectroscopies. Extended X-ray absorption fine structure (EXAFS) spectroscopy was used to characterize the catalyst prepared from $[H_3Re_3(CO)_{12}]$.

Precise structural characterization of surface species with EXAFS requires the use of reference materials in the experimentation and data analysis.[11] Since EXAFS spectroscopy can lead to precise characterization of the metal–support bonds in supported organometallics, these samples are valuable models for the metal–support interface[12] in supported metal catalysts. EX-

[†] University of Delaware.
[‡] Eindhoven University of Technology.

(1) Boudart, M. *Adv. Catal.* **1969**, *20*, 153.
(2) Somorjai, G. A.; Carrazza, J. *Ind. Eng. Chem. Fundam.* **1986**, *25*, 63.
(3) Gault, F. G. *Adv. Catal.* **1981**, *30*, 1, and references therein.
(4) Van Broekhoven, E. H.; Schoonhoven, J. W. F. M.; Ponec, V. *Surf. Sci.* **1985**, *156*, 899.
(5) Crabtree, R. H. *Chem. Rev.* **1985**, *85*, 245, and references therein.
(6) Bergman, R. G. *Science* **1984**, *223*, 902.
(7) Sinfelt, J. H. *Bimetallic Catalysts: Discoveries, Concepts, and Applications*; Wiley: New York, 1983.
(8) Bandy, J. A.; Cloke, G. N.; Green, M. L. H.; O'Hara, D.; Prout, K. *J. Chem. Soc., Chem. Commun.* **1984**, 240.
(9) Baudry, D.; Ephritikhine, M.; Felkin, H. *J. Chem. Soc., Chem. Commun.* **1982**, 606.
(10) Crabtree, R. H.; Dion, R. P. *J. Chem. Soc., Chem. Commun.* **1984**, 1260.
(11) Koningsberger, D. C., Prins, R., Eds.; *X-ray Absorption: Principles, Applications, Techniques of EXAFS, SEXAFS, XANES*; Wiley: New York, 1988.

0022-3654/90/2094-8439$02.50/0

AFS has been used often to characterize conventional supported metal catalysts, which consist of nonuniform aggregates (crystallites) of metal dispersed on high-surface-area porous supports such as metal oxides. Therefore, one of the goals of this research was to prepare a catalyst consisting of supported Re aggregates and to compare its structure and catalytic properties with those of the supported organorhenium catalysts. The following paragraphs are a summary of the synthesis and characterization of a hierarchy of supported rhenium species including (1) mononuclear complexes on MgO formed from $[HRe(CO)_5]$, (2) anionic clusters formed by deprotonation of $[H_3Re_3(CO)_{12}]$ on MgO, (3) ensembles formed by fragmentation of the anionic clusters, and (4) metallic aggregates of Re formed by reduction of the ensembles in hydrogen.

Experimental Methods

Synthesis. The precursor $[H_3Re_3(CO)_{12}]$ was prepared from $[Re_2(CO)_{10}]$ (Strem) by the method of Huggins et al.[13] The infrared spectrum in cyclohexane (2094 m, 2084 w, 2030 vs, 2018 w, 2008 s, 1983 m, 1948 vw cm^{-1}) and the ultraviolet–visible spectrum (255, 303, 345 nm) are in agreement with reported values.[14] The $[H_3Re_3(CO)_{12}]$ reacted with MgO (MCB, ~40 m^2/g, calcined at 700 °C) or γ-Al_2O_3 (Degussa, ~100 m^2/g, calcined at 700 °C) when a dry hexane solution of $[H_3Re_3(CO)_{12}]$ was brought in contact with the solid and stirred for 4 h in a drybox. Periodic monitoring of the solution with infrared spectroscopy showed that complete uptake occurred and gave no indication that any soluble byproducts had formed. The solution was decanted, and the solid was washed exhaustively with dry hexanes to remove any physisorbed $[H_3Re_3(CO)_{12}]$ and then placed under vacuum (10^{-4} Torr) for 4 h to remove physisorbed solvent. The resulting solid was stored under N_2 in a drybox until further use.

The precursor $[HRe(CO)_5]$ was synthesized by a reported method.[15] The observed infrared spectrum in cyclohexane (2015 vs, 2005 m, 1983 vw cm^{-1}) and ultraviolet–visible spectrum (272 nm) are in close agreement with reported values.[14,15] No evidence of unreacted $[Re_2(CO)_{10}]$ in the purified product was observed with either spectroscopic technique. The $[HRe(CO)_5]$ was allowed to react with the metal oxide support, the method being the same as that described for $[H_3Re_3(CO)_{12}]$, except that cyclohexane was used as the solvent. Infrared spectra of the solution taken during the course of the reaction provided no evidence of soluble byproducts and showed that in some cases unreacted $[HRe(CO)_5]$ was present for more than 4 h.

In the standard preparations, the MgO support was pretreated by heating at 700 °C for 10 h under vacuum and then for 1 h in flowing dry O_2, followed by 1 h under vacuum. The vacuum treatment was carried out to remove surface carbonate and formate and a fraction of the hydroxyl groups. The oxygen treatment was carried out to remove anion vacancies that were created during the removal of the surface functional groups; omitting this step gives a MgO surface capable of reducing organic compounds (such as pyridine) to give anion radicals.[16]

Characterization of Supported Catalysts. A combination of characterization techniques was applied. Surface species and species extracted from the surface were characterized with infrared and electronic absorption spectroscopies. EXAFS spectroscopy and X-ray photoelectron spectroscopy were also used to characterize some of the solid samples. Elemental analysis for Re was done by X-ray fluorescence spectroscopy. Details are given in the following paragraphs.

1. Infrared Spectroscopy. In situ infrared experiments were carried out to evaluate the stability and reactivity of the surface species derived from $[HRe(CO)_5]$ and from $[H_3Re_3(CO)_{12}]$. Even catalysts in the working state were examined in a cell that was a flow reactor. Samples consisting of self-supporting wafers (1 cm in diameter) were pressed from the powder at 686 atm and loaded into the infrared cells in the drybox. The gas-handling system, which allowed evacuation and both static and flowing gas treatments, and the quartz sample cells have been described.[17] The spectra were measured with a Nicolet 7199 Fourier transform spectrophotometer with a resolution of 1 cm^{-1}.

2. Reaction and Extraction. The reactivity of the surface-bound complex formed from $[HRe(CO)_5]$ and MgO with water and with various hydrocarbons was investigated by exposing the sample to static pressures (0.1–50 Torr) of each gas while monitoring the changes in the carbonyl region of the infrared spectrum of the solid. Alternatively, extraction of supported organometallics with the various solvents was carried out with 100 mg of solid added to 3 mL of liquid. The solvents employed included methanol, ethanol, isopropyl alcohol, THF, acetonitrile, and methylene chloride with $[(C_6H_5)As][Cl]$, $[(C_6H_5)_4As][Br]$, $[Me_4N][Cl]$, and $[Et_4N][Cl]$. The suspensions were allowed to stand in a drybox, with liquid samples being removed periodically for infrared analysis. Samples were filtered before being placed in the infrared cell (0.202-mm path length).

The reaction with strong acids of the MgO-bound complex formed from $[HRe(CO)_5]$ was investigated by dissolving 1 g of sample in 20 mL (~200% excess with respect to the MgO) of H_3PO_4 at 0 °C. The H_3PO_4 was added dropwise to a 250-mL round-bottom flask containing 20 mL of cyclohexane and the sample at −78 °C. The acid froze immediately upon coming in contact with the solid cyclohexane. The flask was transferred to an ice bath, where it was gently warmed to 0 °C. The reaction was allowed to proceed with vigorous stirring for 24 h. After 8 h all of the MgO had dissolved.

3. Ultraviolet–Visible Spectroscopy. Electronic absorption spectra of the supported Re carbonyls were recorded with a Cary 219 spectrophotometer. Gas-tight quartz sample cells (1-mm path length), loaded in the drybox, were used for both solid (powder) and liquid samples. The spectra of the powder samples were recorded with a diffuse reflectance sphere (Model 40513).

4. X-ray Photoelectron Spectroscopy (XPS). Re oxidation states were estimated by XPS; the instrument was a Physical Electronics AES/XPS Model 550 equipped with a Mg source and a cylindrical mirror analyzer. Details of the experimental methods are described elsewhere.[18]

5. X-ray Fluorescence Spectroscopy. The Re contents of the solid samples were determined by X-ray fluorescence spectroscopy with a Philips automated X-ray spectrometer (PW 1410/85) calibrated with similar standards.

6. EXAFS Spectroscopy. a. Sample Treatment. The structure initially formed from $[H_3Re_3(CO)_{12}]$ on the MgO surface was characterized in the presence of He in a controlled-environment EXAFS cell.[19] The initial sample incorporated adsorbed Re clusters. In the next step of the treatment in the cell, the surface-bound organometallic was decomposed by heating in flowing He (100 mL/min) at 225 °C for 4 h, whereupon the X-ray absorption spectrum was measured again. Then the sample, still in the cell, was brought in contact with flowing H_2 and heated at 5 °C/min to 225 °C, held at this temperature for 4 h, and then heated at 5 °C/min to 350 °C and held for 4 h at this temperature, whereupon the spectrum was again measured. In a separate experiment, a sample initially incorporating the Re cluster anion formed by adsorption of $[H_3Re_3(CO)_{12}]$ was heated at 5 °C/min to 500 °C and held at this temperature for 1 h, whereupon the spectrum was measured. After each step, the sample was held under H_2 at atmospheric pressure as the spectra were collected.

b. EXAFS Measurements. Most of the EXAFS experiments were performed on beamline C-2 at the Cornell High Energy

(12) Duivenvoorden, F. B. M.; Koningsberger, D. C.; Uh, Y. S.; Gates, B. C. *J. Am. Chem. Soc.* **1986**, *108*, 6254.
(13) Huggins, P. K.; Fellman, W.; Smith, J. M.; Kaesz, H. D. *J. Am. Chem. Soc.* **1964**, *86*, 4841.
(14) Epstein, R. A.; Goffney, T. R.; Geoffroy, G. L.; Gladfelter, W. L.; Henderson, R. S. *J. Am. Chem. Soc.* **1979**, *101*, 3847.
(15) Urbansic, M. Ph.D. Dissertation, University of Illinois, 1984; p 75.
(16) Morris, P. M.; Klabunde, K. *Inorg. Chem.* **1983**, *22*, 682.
(17) Barth, R.; Gates, B. C.; Zhao, Y.; Knözinger, H.; Hulse, J. *J. Catal.* **1983**, *82*, 147.
(18) Kirlin, P. A.; Strohmeir, B. R.; Gates, B. C. *J. Catal.* **1986**, *98*, 308.
(19) Kampers, F. W. H., Thesis, Eindhoven University of Technology, The Netherlands, 1988.

TABLE I: EXAFS Analysis: Structural Parameters Characterizing the Reference Compounds and the Ranges in k and r Space Used To Extract the Reference Data

sample	crystallog data: shell	N	R, Å	Fourier transform k^n: n	Δk, Å^{-1}	Δr, Å	ref
Re powder	1st Re–Re	12	2.751	3	2.9–16.4	1.7–3.4	27a
Pt foil	1st Pt–Pt	12	2.770	3	2.5–19.2	1.7–3.4	20a
IrAl alloy	1st Ir–Al	8	2.58	2	3.1–12.0	0.9–2.5[a]	20b
ReO_3	1st Re–O	6	1.867	3	2.5–11.0	0.7–2.1	20c
$[Os_3(CO)_{12}]$[b]	Os–Os	2	2.88				20d
	Os–C[c]	4	1.95	3	2.90–12.4	0.9–2.0	
	Os–O*[c]	4	3.09	3	2.90–12.4	2.0–3.3	

[a] Inverse Fourier transform after subtraction of the Ir–Ir contribution calculated with N = 6, R = 2.99 Å, $\Delta\sigma^2$ = 0.002 Å^2, E_0 = −3.5 eV. [b] Os–C–O angle = 169°. [c] After subtraction of the Os–Os contribution: N = 2, R = 2.88 Å, $\Delta\sigma^2$ = −0.001 Å^2, and E_0 = −3.3 eV, with an inner potential correction of E_0 = −4.4 eV on the difference file.

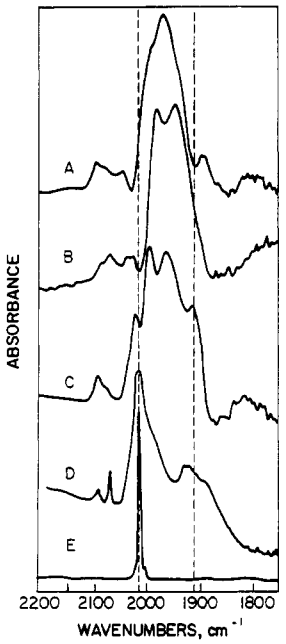

Figure 1. Infrared spectra: (A) MgO-supported species formed by adsorption of $[HRe(CO)_5]$ and inferred to be $\{MgO\}H\cdots[Re(CO)_5]^-$; (B) this species after being brought in contact with methanol at 10 Torr and room temperature followed by evacuation to 10^{-4} Torr; (C) the former species in contact with H_2O at 0.2 Torr and room temperature; (D) in contact with H_2O at 20 Torr and room temperature; (E) $[HRe(CO)_5]$ in cyclohexane at room temperature.

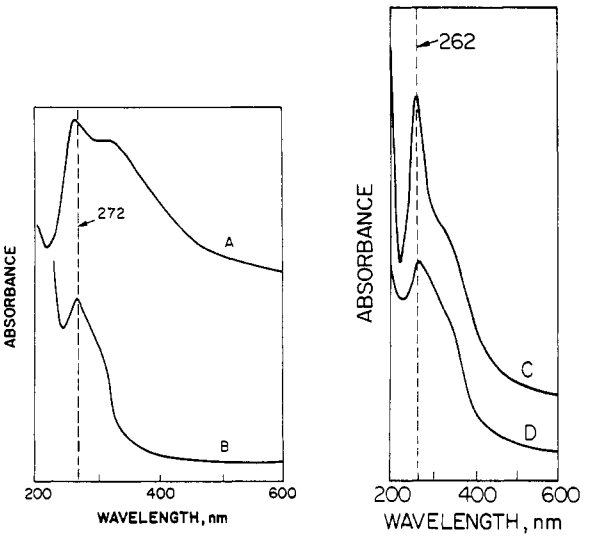

Figure 2. Electronic absorption spectra of surface species inferred to be (A) $\{MgO\}H\cdots[Re(CO)_5]^-$; (B) $[HRe(CO)_5]$ in cyclohexane; (C) the sample of spectrum A following exposure to H_2 at 80 °C for 4 h; (D) $[H_2Re_3(CO)_{12}]^-\{MgO\}$ following exposure to H_2 at 225 °C for 4 h.

Synchrotron Source (CHESS) with a ring energy of 5 GeV and ring currents between 20 and 40 mA. The Si(111) channel cut monochromator was detunable; higher harmonic rejection was obtained by detuning until the intensity of the monochromatic beam had been reduced by 50%. The EXAFS spectra were recorded in the transmission mode with the samples (cooled with liquid nitrogen) at approximately −173 °C. The samples were used in the form of pressed wafers, with the thickness chosen to give $\mu x \approx 2.5$, where μ is the absorption coefficient and x is the sample thickness.

c. Reference Compounds. The EXAFS data analysis was based on experimentally determined phase and amplitude functions of reference compounds with known crystallographic structures (Table I). $[Os_3(CO)_{12}]$ powder (Strem), Re metal powder (Aesar, 99.999%), ReO_3 powder (Alfa), Pt foil (Goodfellows, thickness 4 μm), and IrAl alloy powder were used as references. The Re powder was reduced in flowing H_2 (100 mL/min) at atmospheric pressure and 450 °C for 1 h in an attempt to ensure that it was entirely in the metallic state. The IrAl alloy was prepared by heating $IrCl_3$ and $AlCl_3$.[20b] The X-ray powder diffraction patterns of ReO_3 and IrAl showed only those lines reported for the pure materials. The choices of $[Os_3(CO)_{12}]$ as a reference for Re–CO and of IrAl as a reference for Re–Mg are justified below. The reference powders were diluted with inert boron nitride or with γ-Al_2O_3 powder to give optimal signal-to-noise ratios.[11] The EXAFS spectra were recorded with the samples at approximately −173 °C, except for ReO_3, which was characterized at room temperature.

Some reference compounds were also characterized by EXAFS spectroscopy on beam line X-11-A at the National Synchrotron Light Source (NSLS) at Brookhaven National Laboratory with a double crystal Si(111) monochromator, which was detuned to 50% of the primary intensity. Internal cross checks showed no amplitude differences greater than 10%. Another standard, $[Os_3(CO)_{12}]$, was characterized at the Stanford Synchrotron Radiation Laboratory, as described elsewhere.[12]

Results and Discussion

Reactions of Catalyst Precursors with the MgO Surface. In the first step in each catalyst synthesis, the organometallic precursor, $[HRe(CO)_5]$ or $[H_3Re_3(CO)_{12}]$, in hydrocarbon solution was brought in contact with the MgO support. The resulting surface organometallic species (the catalyst precursors) were characterized spectroscopically and by wet chemistry; the details are presented below.

1. Chemisorption of $[HRe(CO)_5]$ To Form $\{MgO\}H^+\cdots[Re(CO)_5]^-$. The infrared spectrum of the species resulting from the interaction of $[HRe(CO)_5]$ with the MgO surface exhibits one strong band that is considerably broadened (typical of metal oxide supported organometallics) relative to that of $[HRe(CO)_5]$ in cyclohexane (Figure 1). In addition, the infrared spectrum of the supported Re carbonyl is red-shifted relative to this solution spectrum, with the major peak appearing at a frequency inter-

(20) (a) Wyckoff, R. W. G. *Crystal Structures I*, 2nd ed.; Wiley: New York, 1963; pp 10–11. (b) Esslinger, R.; Schubert, K. *Z. Metallk.* **1957**, *48*, 126. (c) Wyckoff, R. W. G. *Crystal Structures II*, 2nd ed.; Wiley: New York, 1963; p 52. (d) Corey, E. R.; Dahl, L. F. *Inorg. Chem.* **1962**, *1*, 521.

mediate between those characteristic of $[HRe(CO)_5]$ and $[Re(CO)_5]^-$.[21] The ultraviolet–visible spectrum of the supported complex agrees with that of $[HRe(CO)_5]$ in cyclohexane (Figure 2), the lack of bands characteristic of Re–Re bonds ($\lambda > 330$ nm) being consistent with the inference that condensation to give Re clusters had not occurred.

The changes in the infrared spectrum upon adsorption of the mononuclear Re complex can be interpreted in terms of ion pairing with the MgO surface. The partial deprotonation of $[HCo(CO)_4]$ by NR_3 in solution[22] is similar to the partial deprotonation of $[HRe(CO)_5]$ on the MgO surface. In the solid state, the structure of $[R_3NH^+Co(CO)_4]^-$ shows interaction of the proton with the cobalt center, i.e., contact ion pairing.[22] Consequently, the overall symmetry of the carbonyl ligands about the Co center is maintained, C_{3v}. Similarly, upon adsorption of $[HRe(CO)_5]$ on MgO, the symmetry of the Re carbonyl remains C_{4v}.[23] The red shift in the infrared spectrum of the supported complex relative to that of $[HRe(CO)_5]$ in cyclohexane suggests a partial deprotonation of the mononuclear rhenium hydride.

Coadsorption of polar ligands on MgO (MeOH, EtOH, *i*-PrOH, THF, CH_3CN, CH_2Cl_2) with $[HRe(CO)_5]$ changed the spectrum of the surface-bound organometallic species to one that agrees, in both the relative intensities and number of bands, with that of $[Re(CO)_5]^-$.[24] This result can be explained by separation of ion pairs by the polar ligands that act like solvents on the MgO surface. The basic surface partially deprotonates the rhenium hydride. An interaction of the proton with the Re center, however, is maintained. The polar ligands are able to "solvate" the proton, thus effectively removing H^+ from the Re coordination sphere. The $[Re(CO)_5]^-$ relaxes to a trigonal bipyramid geometry, consistent with the interpretation of the infrared spectrum.

Exposure of the surface species $\{MgO\}H^+\cdots[Re(CO)_5]^-$ to 10 Torr of methanol gave an infrared spectrum (Figure 1B) corresponding to $[Re(CO)_5]^-$. Similar results were obtained with other polar compounds such as THF and water (Figure 1C). The infrared spectra of these species are consistent with the molecular symmetry of the pentacarbonylrhenate anion, but the spectrum of the surface-bound complex is blue-shifted relative to that of $[Re(CO)_5]^-$ in solution. This result implies that either the Re is still only partially deprotonated or that the MgO surface is able to delocalize some of the charge away from the rhenium carbonyl ligands.

On the basis of these results, an attempt was made to extract $[Re(CO)_5]^-$ from the MgO surface by cation metathesis with polar solvents containing quaternary ammonium and arsonium salts. No organometallic species were observed in the infrared spectra of the solution when the solids had loadings less than 2 wt % Re. Similar results were obtained with nonpolar solvents. However, when the loadings were greater than 2 wt % Re, the solid became orange-pink, and $[HRe_2(CO)_9]^-$, identified by its infrared spectrum, could be extracted from the surface.[25] It is known that the complex $[Re(CO)_5]^-$ is unstable (cf. ref 21). It is possible that the observation of $[Re(CO)_5]^-$ as an extracted product was precluded by the lapse of time between the extraction and the recording of the spectrum. Further, the choice of solvent may contribute to the formation of the $[HRe_2(CO)_9]^-$. The solvents used in the extraction have relatively low pK_a's and could provide the proton for the dinuclear complex.

Contacting of $\{MgO\}H^+\cdots[Re(CO)_5]^-$ with high partial pressures of water was effective in generating $[HRe(CO)_5]$ (Figure 1D). A small quantity of $[Re_2(CO)_{10}]$ was also formed, as evidenced by the weak band at 2070 cm^{-1}. Only small amounts of $[HRe(CO)_5]$ were observed upon dosing with methanol. The $[HRe(CO)_5]$ could then be removed from the surface by evacuation at 1 Torr, as determined by the disappearance of the band at 2015 cm^{-1} in the infrared spectrum. Similarly, dissolving the $\{MgO\}H^+\cdots[Re(CO)_5]^-$ in H_3PO_4 at 0 °C liberated $[HRe(CO)_5]$, which was trapped in a cyclohexane layer above the acid, as determined by infrared spectroscopy. No other organorhenium species were observed in the organic layer above the H_3PO_4. The reactivity of $\{MgO\}H^+\cdots[Re(CO)_5]^-$ with acids parallels that of the pentacarbonyl rhenate in solution, which is also protonated by H_2O or H_3PO_4 to give $[HRe(CO)_5]$.

In summary, these results demonstrate that large, sterically hindered cations in solution are not reactive to displace the pentacarbonyl rhenate from the surface. Stronger Brønsted acids than $[HRe(CO)_5]$ can displace the Re carbonyl from the surface.

An attempt was made to extend the surface organometallic chemistry of $[HRe(CO)_5]$ to a less basic metal oxide surface. Substituting γ-Al_2O_3 for MgO in the preparation resulted in negligible uptake of the Re complex from the solution, as determined by infrared and X-ray fluorescence spectroscopy of the resulting solid after it had been evacuated for 4 h to remove any physisorbed $[HRe(CO)_5]$. Evidently, more strongly basic sites than those on the γ-Al_2O_3 surface[26] are required for the chemisorption of $[HRe(CO)_5]$.

These results obtained for the mononuclear hydridorhenium carbonyl complex supported on MgO are comparable to those reported for the MgO-supported complex formed from $[H_2Os(CO)_4]$.[27] The mononuclear Os complex also interacts strongly with MgO, and the shifts in the infrared spectrum of the metal carbonyl upon adsorption are similar to those stated above for the partially deprotonated Co and Re complexes. However, in contrast to the reactivity observed for $\{MgO\}H^+\cdots[Re(CO)_5]^-$, cation metathesis could be effected, with $[HOs(CO)_4]^-$ being extracted into a solution of $[Me_4N][Cl]$ in THF.[27] Evidently $[H_2Os(CO)_4]$ is ionized to a greater extent by the MgO surface than is $[HRe(CO)_5]$. This conclusion is consistent with the pK_a values of these Os and Re hydrides (15.2[28] and 21.4,[29] respectively). Also, on the basis of the appearance of a low-energy band in the infrared spectrum, an interaction of the oxygen atoms of the carbonyl ligands of the supported Os complex with surface cations (Lewis acid sites) was postulated.[27] No evidence for this bifunctional interaction was found with $\{MgO\}H^+\cdots[Re(CO)_5]^-$. This result suggests that the carbonyl oxygens of the surface-bound Re species may be less basic than those of adsorbed Os carbonyl, which supports the interpretation that the extent of deprotonation is less with the Re complex.

2. Chemisorption of $[H_3Re_3(CO)_{12}]$ *To Give* $[H_2Re_3(CO)_{12}]^-\{MgO\}$. The results of experiments providing a comparison of the infrared and ultraviolet–visible spectra of the supported species resulting from of the interaction of $[H_3Re_3(CO)_{12}]$ and the MgO surface with the spectra of $[(C_6H_5)_4As][H_2Re_3(CO)_{12}]$ demonstrate that the hydridocarbonyl cluster is quantitatively deprotonated by the MgO.[30] This result is confirmed by EXAFS spectra, as described below. The surface-bound anion $[H_2Re_3(CO)_{12}]^-$ was extracted from the surface by cation metathesis, with $[Et_4N][Cl]$, for example, and characterized spectroscopically in solution. The more facile deprotonation of $[H_3Re_3(CO)_{12}]$ than of $[HRe(CO)_5]$ and of $[H_2Os(CO)_4]$ by the MgO is attributed to the greater acidity of the cluster ($pK_a = 3.5$[23]), which contains bridging hydride ligands.

3. Reactivity of Surface-Bound Complexes To Form $[Re(CO)_3\{OMg\}L_2]$. On the basis of infrared, Raman, ultraviolet–visible, and inelastic electron tunneling spectroscopy, it has been concluded[30] that heating $[H_2Re_3(CO)_{12}]^-\{Mg\}$ to 225 °C for 4 h in H_2 or He or under vacuum (10^{-4} Torr) gives mononuclear complexes, suggested to be $[Re(CO)_3\{OMg\}\{HO\text{-}Mg\}_2]$. The exact

(21) Ellis, T. E.; Flom, E. A. *J. Organomet. Chem.* **1975**, *99*, 263.
(22) Calderazzo, F.; Fachinetti, G.; Marchetti, F. *J. Chem. Soc., Chem. Commun.* **1981**, 181.
(23) Kaesz, H. D. *J. Organomet. Chem.* **1980**, *200*, 145.
(24) Ziegler, T. *Organometallics* **1985**, *4*, 675.
(25) Ciani, G.; D'Alfonso, G.; Freni, M.; Romiti, P.; Sironi, A. *J. Organomet. Chem.* **1978**, *157*, 199.
(26) Tanabe, K. *Solid Acids and Bases*; Academic Press: New York, 1970.
(27) Lamb, H. H.; Gates, B. C. *J. Am. Chem. Soc.* **1986**, *108*, 81.
(28) Walker, H. W.; Pearson, R. G.; Ford, P. C. *J. Am. Chem. Soc.* **1983**, *105*, 1179.
(29) Martin, B. D.; Warner, K. E.; Norton, J. R. *J. Am. Chem. Soc.* **1986**, *108*, 33.
(30) Kirlin, P. S.; DeThomas, F. A.; Bailey, J. W.; Gold, H. S.; Dybowski, C.; Gates, B. C. *J. Phys. Chem.* **1986**, *90*, 4882.

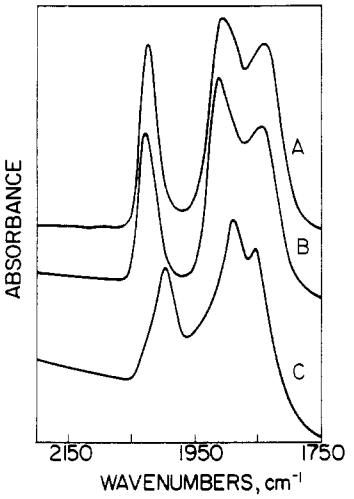

Figure 3. Infrared spectra taken at room temperature of (A) sample inferred to be $\{MgO\}H\cdots[Re(CO)_5]^-$ after exposure to H_2 at 80 °C for 4 h; (B) $[H_2Re_3(CO)_{12}]\{MgO\}$ after exposure to H_2 at 225 °C for 4 h; (C) solid sample formed by bringing $[H_3Re_3(CO)_{12}]$ in THF solution in contact with MgO.

SCHEME I: Chemistry of Rhenium Carbonyls on the Surface of MgO

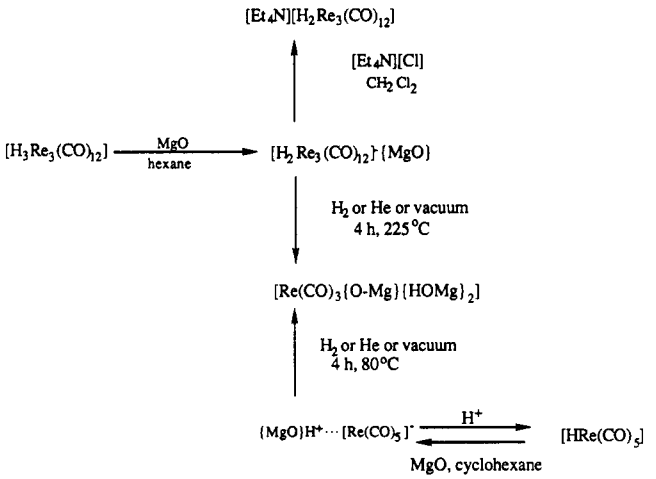

identities of the noncarbonyl ligands remain to be determined, but it is evident from the symmetry that there are two kinds, inferred to be oxo and hydroxo.[31]

The stability of the complex formed from $[HRe(CO)_5]$, $\{MgO\}H^+\cdots[Re(CO)_5]^-$, has also been investigated at elevated temperatures. The infrared spectra obtained by heating $\{MgO\}H^+\cdots[Re(CO)_5]^-$ to 80 °C under H_2, He, or vacuum are indistinguishable from the spectrum obtained for the sample prepared from $[H_2Re_3(CO)_{12}]^-\{Mg\}$ at 225 °C[30] (Figure 3). The ultraviolet–visible spectra show similar agreement (Figure 2). These results demonstrate that $[Re(CO)_3\{OMg\}\{HOMg\}_2]$ is formed from $\{MgO\}H^+\cdots[Re(CO)_5]^-$ under conditions that are less severe than those required for the sample prepared from the trinuclear cluster. The difference in reactivity may be attributed to the stability provided by the metal–metal bonds in the cluster. The surface chemistry is summarized in Scheme I.

4. Interaction of CO with Supported Re Crystallites. Samples prepared from $[H_3Re_3(CO)_{12}]$ on MgO were treated in H_2 to give Re crystallites dispersed on the support. The samples containing the Re crystallites were characterized by infrared spectroscopy after exposure to CO at room temperature (Figure 4A). The result is interpreted as the superposition of the spectrum of CO

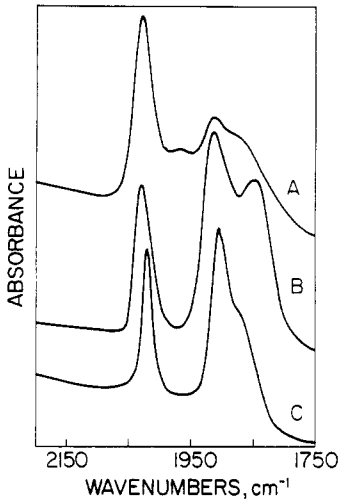

Figure 4. Infrared spectra taken at room temperature of (A) Re crystallites on MgO, poisoned with CO at 25 °C; (B) surface structure inferred to be $[Re(CO)_3\{OMg\}\{HOMg\}_2]$; (C) sample formed from MgO-supported Re crystallites after contacting with CO at 225 °C.

linearly bound to the surface atoms of Re metal[32] and the spectrum of $[Re(CO)_3\{OMg\}\{HO\text{-}Mg\}_2]$ (Figure 4B).

A different spectrum resulted from CO adsorption on the MgO-supported Re crystallites at 225 °C (Figure 4C); this spectrum is virtually indistinguishable from that of the Re subcarbonyl (Figure 4B). These results suggest that in addition to occupying sites on the metal surface, CO at elevated temperatures can induce major structural changes, leading to the complete oxidative fragmentation of the metal crystallites. These results are consistent with those reported for small Rh crystallites supported on γ-Al_2O_3, which demonstrate that the metal is converted to $Rh(CO)_2\{OAl\}_j\{HOAl\}_k$ (where j and k are integers ranging from 0 to 3) by reaction with CO at 25 °C.[33] The more facile reaction of the Rh than of the Re to give the subcarbonyl may be attributed to the higher dispersion of the Rh catalysts and to the lower metal–metal bond strength of the Rh.[34,35]

5. Characterization of Surface Structures by EXAFS Spectroscopy. a. Data Reduction. The EXAFS data were obtained from each experimental X-ray absorption spectrum by a cubic spline background subtraction[36] and were normalized by division by the edge height.[37] The raw data characterizing the samples prepared from $[H_3Re_3(CO)_{12}]$ adsorbed on MgO and the data characterizing the reference compounds, together with their k^n-weighted Fourier transforms, are shown in Figures 5 and 6, respectively. The data quality is high for samples containing such a low concentration of Re (2.2 wt %). For example, Figure 5A,C shows signal-to-noise ratios > 120 at k = 3 Å^{-1}. The high signal-to-noise ratios characterizing the reference compound data make it possible to obtain phase shift and backscattering amplitudes reliably over a wide range of the wave factor k.

b. Reference Compounds. Only experimentally determined phase shifts and backscattering amplitudes were used in the data analysis.[37] The ranges used for the Fourier transformations and

(31) The two donor {HOMg} ligands were identified only by inference. Other ligands, such as $\{OMg_2\}$, cannot be excluded on the basis of the available evidence; what is clear is that two of the noncarbonyl ligands are different from the third.

(32) The infrared spectrum of CO linearly bound to supported Re crystallites has been reported to have one strong band at 2035 cm^{-1}: Bolivar, C.; Charcosset, H.; Frety, R.; Primet, M.; Rournayan, L.; Betizeau, C.; Leclercq, C.; Maurel, R. *J. Catal.* **1976**, *45*, 163.

(33) van't Blik, H. F. J.; van Zon, J. B. A. D.; Huizinga, T.; Vis, J. C.; Koningsberger, D. C.; Prins, R. *J. Am. Chem. Soc.* **1985**, *107*, 3139. Zaki, M. I.; Kunzmann, G.; Gates, B. C.; Knözinger, H. *J. Phys. Chem.* **1987**, *91*, 1486.

(34) The standard free energy of sublimation of rhenium ($\Delta G°_f$ = 749 kJ/mol) is much larger than that of rhodium ($\Delta G°_f$ = 532 kJ/mol): Weast, R. C., Ed. *Handbook of Chemistry and Physics*; The Chemical Rubber Co.: Cleveland, 1972; p D69.

(35) The hydroxyl groups may also play a role in the mechanism of the breakup of the metal particles.

(36) Cook, J. W.; Sayers, D. E. *J. Appl. Phys.* **1981**, *52*, 5024.

(37) van Zon, J. B. A. D.; Koningsberger, D. C.; van't Blik, H. F. J.; Sayers, D. E. *J. Chem. Phys.* **1985**, *82*, 5742.

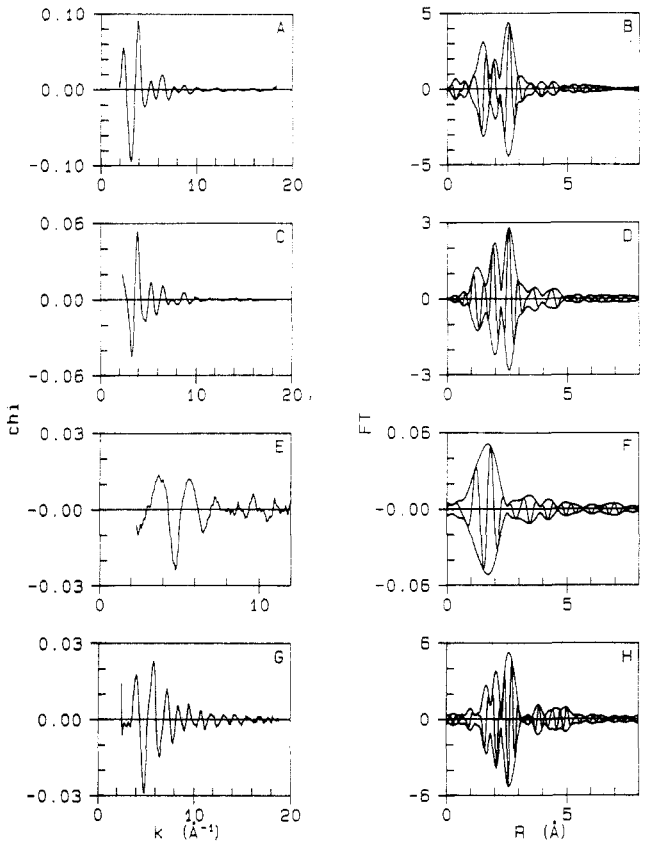

Figure 5. (A) Raw EXAFS data and (B) Fourier transform (k^3-weighted, Δk = 2.8–11.5 Å^{-1}) of a sample prepared by adsorption of $[H_3Re_3(CO)_{12}]$ on MgO; (C) raw EXAFS data and (D) Fourier transform (k^3-weighted, Δk = 2.8–11.5 Å^{-1}) of sample following oxidative fragmentation of the adsorbed trirhenium clusters; (E) raw EXAFS data and (F) Fourier transform (k^1-weighted, Δk = 3–9 Å^{-1}) of sample after treatment in hydrogen at 350 °C; (G) raw EXAFS and (H) Fourier transform (k^3-weighted, Δk = 2.5–14 Å^{-1}) of sample after treatment in hydrogen at 500 °C.

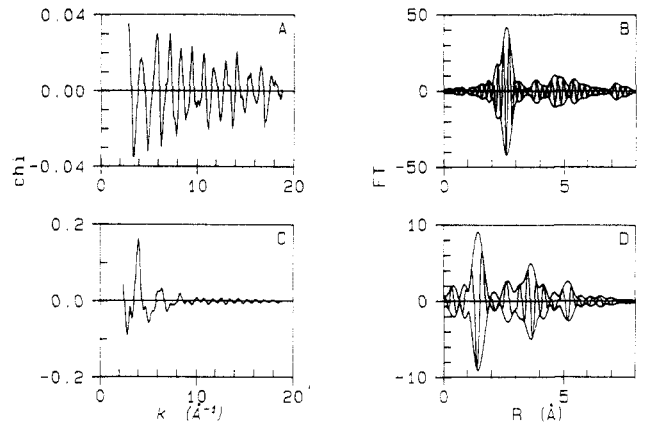

Figure 6. (A) Raw EXAFS data and (B) Fourier transform (k^3-weighted, Δk = 2.9–16.4 Å^{-1}) of Re powder; (C) raw EXAFS data and (D) Fourier transform (k^3-weighted, Δk = 2.5–11 Å^{-1}) of ReO_3.

inverse Fourier transformations to create the reference data files are given in Table I. The Re–Re and Re–O references were taken from the first-shell data for the Re powder and ReO_3, respectively.

The IrAl alloy was used as a reference for the Re–Mg absorber–scatterer pair. The absorbers (Ir and Re) and the scatterers (Al and Mg) are near neighbors in the periodic table. The differences in phase shifts and backscattering amplitudes between these neighbors have been shown both experimentally[12,38] and theoretically[39] to be small, allowing a transferability of the phase

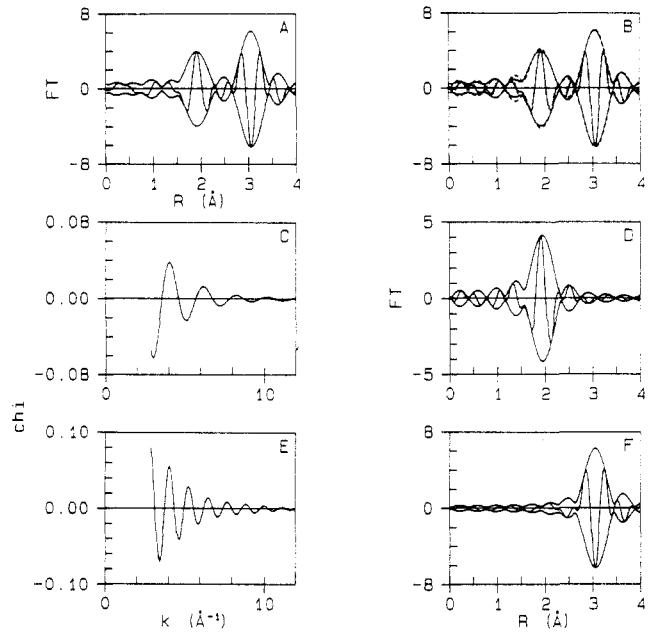

Figure 7. Details of construction of Os–C and Os–O* EXAFS reference data: (A) Fourier transform (k^3-weighted, Δk = 2.9–12.4 Å^{-1}) of difference file (data minus calculated Os–Os contribution) with ΔE_0 = −4.4 eV, representing the Os–C–O* EXAFS; (B) Fourier transform (k^3-weighted, Δk = 3.7–11.9 Å^{-1}, Os–O phase corrected) of difference file (solid line) and isolated (Δr = 0.9–3.3 Å) Os–C–O* contribution (dashed line); (C) isolated Os–C reference EXAFS, with (D) Fourier transform (k^3-weighted, Δk = 3.7–11.9 Å^{-1}, Os–O phase corrected); (E) isolated Os–O* reference EXAFS, with (F) Fourier transform (k^3-weighted, Δk = 3.7–11.9 Å^{-1}, Os–O phase corrected).

shifts and backscattering amplitudes. In the determination of the Ir–Al EXAFS reference from the IrAl alloy EXAFS data, it was essential first to subtract the first-shell Ir–Ir contribution from the data. The details of the determination of this reference are given elsewhere.[40]

It was essential to select a good reference for the Re–CO contributions, with structural similarity between the reference compound and the sample being a primary criterion. Since the multiple scattering effect in the Re–O* shell (O* refers to the oxygen of a carbonyl ligand) is significant,[41] it was judged necessary to fit with a Re–O reference that exhibits multiple scattering.[42] $[Os_3(CO)_{12}]$ was the choice, since (1) its structure is well-known,[20d] (2) its structure is very similar to those of $[H_xRe_3(CO)_{12}]^{x-3}$ (x = 1–3),[42,43] and (3) Os is a near neighbor of Re in the periodic table. A straightforward isolation of the Os–C and Os–O* contributions was not possible because the Os–O* contribution shows overlap with the Os–Os contribution in r space. The Os–Os contribution was determined by a procedure described elsewhere.[12] On the basis of the crystallographic values for the Os–Os coordination[20d] (N_{Os-Os} = 2, R = 2.88 Å), an Os–Os EXAFS was calculated with $\Delta\sigma^2$ = −0.001 Å^2 and E_0 = −3.3 eV by using the phase shift and backscattering amplitude obtained from the data for Pt foil.[20a] The calculated Os–Os EXAFS was subtracted from the EXAFS data, and the difference file was Fourier transformed (with no phase or amplitude correction) over the widest possible range in k space giving reliable results (Figure 7A). To separate the Os–C and the Os–O* contributions from the difference spectrum, the Os–C and Os–O* peaks in Figure 7A were inverse Fourier transformed by using the windows shown in the figure. The phase and backscattering amplitudes—now

(38) Lengeler, B. *J. Phys. (Paris) C8*, **1986**, *47*, 75.
(39) Teo, B. K.; Lee, P. A. *J. Am. Chem. Soc.* **1979**, *101*, 2815.
(40) van Zon, F. B. M.; Van Gruijthuijsen, L. M. P.; Koningsberger, D. C., to be published.
(41) Teo, B. K. *J. Am. Chem. Soc.* **1981**, *103*, 3990.
(42) van Zon, F. B. M.; Kirlin, P. S.; Gates, B. C.; Koningsberger, D. C. *J. Phys. Chem.* **1989**, *93*, 2218.
(43) Ciani, G.; D'Alfonso, G.; Freni, M.; Romiti, P.; Sironi, A. *J. Organomet. Chem.* **1978**, *157*, 193.

ready to be used for independent analysis of the Re–C and Re–O* contributions—are reliable in the range $3.7 < k < 11.9$ Å^{-1}. The demonstration of this reliability is provided by the results of Figure 7B, where the Fourier transforms of the EXAFS characterizing the isolated data and the original difference file are shown for the above-mentioned range in k space. Both the magnitudes and the imaginary parts coincide almost completely. It is evident from this figure that the imaginary part of the Os–C contribution peaks positively in a Pt–O phase-corrected Fourier transform, whereas the phase of the imaginary part of the Os–O* peak is shifted approximately π rad with respect to the Os–C peak as a consequence of the multiple scattering effect. The isolated Os–C EXAFS is shown in Figure 7C; the corresponding phase-corrected Fourier transform is shown in Figure 7D. The imaginary part is still almost symmetric, with small deviations associated with the isolation procedure. The Os–O* EXAFS, with its phase-corrected Fourier transform, is shown in Figure 7E,F. The imaginary part is again symmetric and peaks negatively—just as for the same peak in Figure 7B. We conclude from these results that the Os–C and Os–O* contributions can be separated reliably from the $[Os_3(CO)_{12}]$ EXAFS function and can be used to analyze independently the Re–C and Re–O* EXAFS contributions characterizing the supported rhenium carbonyls.

c. Supported Rhenium Carbonyls. The data analysis was performed with phase-corrected Fourier transforms. The use of such transforms aids in the attribution of the peaks in r space to shells of the proper neighbors.[12,37] For example, with a Re–Re phase correction, the imaginary part of the Re–Re contribution peaks positively, and with a Re–O phase correction, the imaginary part of the Re–C contribution peaks positively and that of the Re–O* contribution peaks negatively (as a consequence of the multiple scattering effect in the M–O* shell of metal carbonyls).[41,42]

i. Adsorption of $[H_3Re_3(CO)_{12}]$ on MgO. The difference file technique[12,37] was used in the analysis of the EXAFS data characterizing the surface species initially formed by adsorption of $[H_3Re_3(CO)_{12}]$ on MgO. First, a Re–C contribution was calculated that agreed as well as possible with the Re–C peak of the data in a Re–O phase-corrected k^3-weighted Fourier transform. In this part of the analysis, the Re–C coordination was fixed at a value of four neighbors around Re, consistent with the absence of a loss of CO ligands upon adsorption of $[H_3Re_3(CO)_{12}]$. This Re–C contribution was then subtracted from the data, and fitting was done to find coordination parameters for the combined Re–O* + Re–Re peak. As a first guess, a Re–O* contribution was calculated with N, $\Delta\sigma^2$, and E_0 equal to the values in the Re–C contribution and with a coordination distance that resulted in the best agreement with the imaginary part of the experimental peak in r space. After subtraction of this first-guess Re–O* contribution, the best Re–Re parameters were determined with a fixed value of two Re neighbors per Re atom, consistent with the trinuclear metal framework of the supported cluster. Subsequently, all three contributions were added and compared by using the data in k space and in r space after a k^3-weighted Fourier transformation.

As usual, such a first cycle in the difference file technique did not yield the best agreement possible, and therefore the previously calculated Re–O* and Re–Re contributions were subtracted from the data, and better parameters were sought. It was not possible to obtain acceptable agreement in both k space and r space when only the Re–C, Re–O*, and Re–Re contributions were accounted for. Therefore, the analysis was improved by the inclusion of contributions from the support, namely, those associated with the O and Mg.

The use of phase-corrected Fourier transforms is crucial in this case. The phase shift of the Re–O contribution is much different (by approximately π rad) from that of the Re–Mg absorber–scatterer combination[39] and can therefore be used readily to discriminate between O and Mg scatterers. The subsequent steps in the analysis by the difference file technique of the data characterizing the supported cluster anion are shown in Figure 8. It is evident from an examination of the difference file obtained

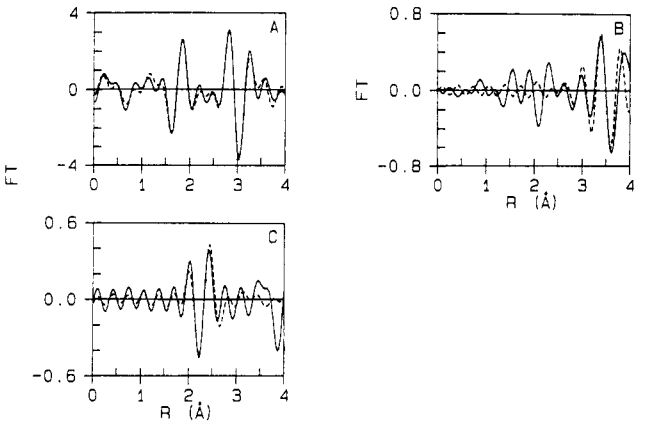

Figure 8. Illustration of the subsequent steps used in the difference file technique for the analysis of EXAFS data characterizing the sample formed from adsorption of $[H_3Re_3(CO)_{12}]$ on MgO. The imaginary parts of Fourier transforms are taken with k^3 weighting and $\Delta k = 3.6$–9.8 Å^{-1}. (A) Experimental (solid line) and calculated (dashed line) Re–C + Re–O* EXAFS, Re–O phase corrected; (B) experimental minus calculated Re–C + Re–O* EXAFS (solid line) and calculated Re–Re EXAFS (dashed line), Re–Re phase corrected; (C) experimental minus calculated Re–C + Re–O* + Re–Re EXAFS (solid line) and calculated Re–Mg EXAFS (dashed line), Re–Mg phase corrected.

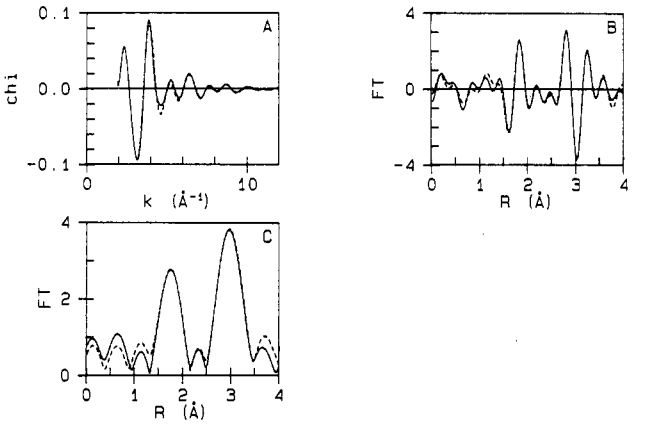

Figure 9. EXAFS analysis results obtained with the best calculated coordination parameters for the sample prepared by adsorption of $[H_3Re_3(CO)_{12}]$ on MgO; (A) experimental EXAFS (solid line) and sum of the calculated Re–C, Re–O*, Re–Re, and Re–Mg contributions (dashed line); (B) imaginary part and (C) magnitude of the Fourier transform (k^3-weighted, $\Delta k = 3.6$–9.8 Å^{-1}, Re–O phase corrected) of experimental EXAFS and sum of calculated Re–C, Re–O, Re–Re, and Re–Mg contributions.

after subtraction of the Re–C + Re–O* contribution from the data (Figure 8B) that another scatterer (in addition to a detectable Re–Re contribution) is present, as indicated by the peak near 2.2 Å. Application of a Re–Mg phase-corrected Fourier transform to the difference file obtained by subtraction from the experimental EXAFS of the sum of the Re–C, Re–O*, and Re–Re contributions resulted in a positively peaking imaginary part demonstrating the presence of a Mg neighbor (Figure 8C). The Re–C, Re–O*, Re–Re, and Re–Mg contributions to the EXAFS spectrum of this sample were calculated with the best parameters and added. The agreement of the data with this sum in k and in r space is shown in Figure 9. These best parameters are summarized in Table II.

In this analysis and the others that follow, an estimate of the number of statistically allowed adjustable parameters in the fit was made by the following standard criterion: $N = 2\Delta k\Delta r/\pi$, where Δk and Δr are the k and r ranges used in the forward and inverse Fourier transformations. The number of allowed parameters in this analysis is 22 ($\Delta k = 8.7$ Å^{-1}; $\Delta r = 4$ Å); the number of parameters estimated was 16 (Table II).

ii. Surface Species Formed after Heating of the Adsorbed Cluster. The first-shell region ($0 < r < 4$ Å) of the Fourier

TABLE II: EXAFS Results Characterizing the Sample Formed from Adsorption of $[H_3Re_3(CO)_{12}]$ on MgO

shell	N^*	N^a	R, Å	$\Delta\sigma^2$, Å^2	ΔE_0, eV	EXAFS ref
Re–C	4	4	1.912	0.0031	5	Os–C
Re–O*	4	4	3.089	0.0030	5	Os–O*
Re–Re	1.6	2	3.455	0.0010	−10	Re–Re
Re–Mg	0.65	0.65	2.385	0	10	Ir–Al

[a] Coordination numbers N are chosen according to the $[H_2Re_3(CO)_{12}]^-${MgO} model with a bridging Re–Mg–Re ligand. EXAFS analysis was done with coordination numbers $N^* = N\exp[-2(R - R_{ref})/\lambda]$ with $\lambda = 6$ Å.

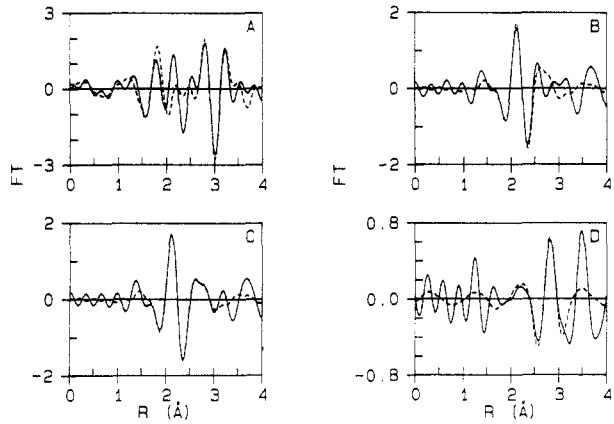

Figure 10. Illustration of the subsequent steps used in the difference file technique for analysis of the EXAFS data characterizing the sample formed from adsorption of $[H_3Re_3(CO)_{12}]$ on MgO following oxidative fragmentation of the supported trirhenium cluster. Imaginary parts of Fourier transform taken with k^3 weighting and $\Delta k = 3.6$–10.4 Å^{-1}: (A) experimental (solid line) and calculated Re–C + Re–O* contribution (dashed line), Re–O phase corrected; (B) experimental minus calculated Re–C + Re–O* contribution (solid line) and calculated $Re–O_{support}$ EXAFS (dashed line), Re–O phase corrected; (C) experimental minus calculated Re–C + Re–O* + $Re–Mg_{support}$ contribution (solid line) and calculated $Re–O_{support}$ EXAFS (dashed line), Re–O phase corrected; (D) experimental minus calculated Re–C + Re–O* + $Re–O_{support}$ contribution (solid line) and calculated $Re–Mg_{support}$ EXAFS (dashed line), Re–Mg phase corrected.

transform characterizing the broken-up cluster formed by heating the initial species formed by adsorption of $[H_3Re_3(CO)_{12}]$ on MgO was analyzed by the same procedure described for the adsorbed species. No evidence was found for a Re–Re coordination characteristic of a triangular rhenium framework. However, it is evident from Figure 10A that now other strong contributions are present in the region $2 < r < 2.7$ Å. These contributions also interfere strongly with the right-hand side of the imaginary part associated with the Re–C peak. Subtracting the EXAFS calculated for Re–C + Re–O* from the EXAFS data showed that two additional contributions must be present in the region $2 < r < 3$ Å. Application of Re–O and Re–Mg phase-corrected Fourier transforms indicated the presence of both an O and a Mg scatterer (Figure 10B–D). The final results are shown in Figure 11, and the best values of the parameters in Table III. The statistically justified number of adjustable parameters was 22 ($\Delta k = 8.7$ Å^{-1}, $\Delta R = 4$ Å); the number of parameters estimated was 16.

There is evidence[44] that the stable MgO(100) face comprises most of the MgO surface. It is therefore well possible that the adsorption sites for Re after cluster decomposition are almost uniquely defined, and thus we suggest that the higher shell distances characterizing the broken-up cluster may be very well defined. Thus, it is of interest not only to investigate the presence of Re neighbors originating from the original Re cluster but also to investigate the higher shell neighboring atoms of the support (O and Mg). Since the number of freely adjustable parameters becomes too large to allow straightforward fitting, it is necessary

(44) Henrich, V. C. *Rep. Prog. Phys.* **1985**, *48*, 1481.

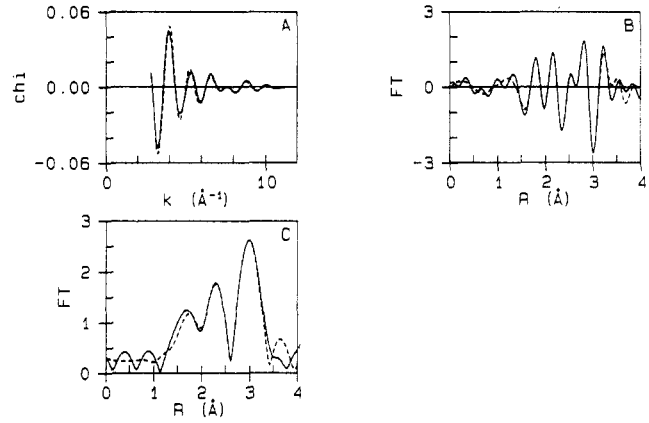

Figure 11. Results of EXAFS analysis obtained with the best calculated coordination parameters for the sample prepared by adsorption of $[H_3Re_3(CO)_{12}]$ on MgO followed by oxidative fragmentation of the supported trirhenium cluster: (A) experimental EXAFS (solid line) and sum of the calculated Re–C + Re–O* + $Re–Mg_{support}$ + $Re–O_{support}$ contributions (dashed line); (B) imaginary part and (C) magnitude of Fourier transform (k^3 weighted, $\Delta k = 3.6$–10.4 Å^{-1}, Re–O phase corrected) of experimental EXAFS (solid line) and sum of the calculated Re–C + Re–O* + $Re–Mg_{support}$ + $Re–O_{support}$ contributions (dashed line).

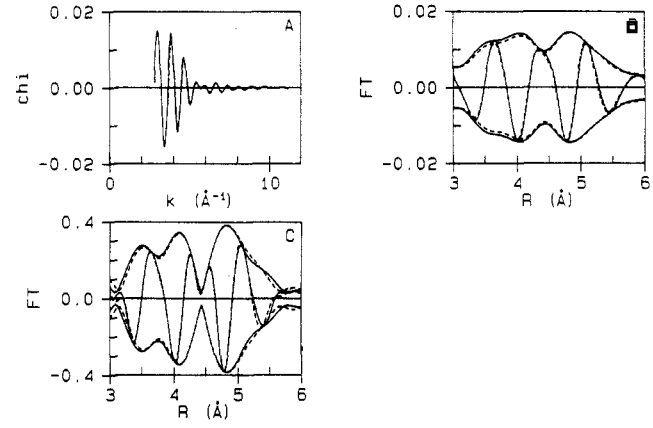

Figure 12. Results of EXAFS analysis of the higher coordination shells of surface structure formed by oxidative fragmentation of the supported trirhenium cluster: (A) experiment (EXAFS characterizing the higher coordination shell obtained after forward (k^3 weighted, $\Delta k = 2.8$–11.3 Å^{-1}) and inverse ($\Delta r = 3.1$–5.2 Å). Fourier transformation (solid line) and calculated (Table V) higher shell contributions (dashed line); (B) imaginary parts and (C) magnitude of Fourier transforms ($\Delta k = 3.6$–9.9 Å^{-1}) of higher shell EXAFS (solid line) and calculated higher shell contributions (dashed line) (B, k^1 weighted; C, k^3 weighted).

to draw some preliminary inferences by constructing models of possible surface species. Various models were considered with tentative analyses of the higher shells present in the Fourier transform of the data.

The EXAFS characterizing the higher coordination shells with distances ranging from 3 to 6 Å was obtained by Fourier transformation (k^3 weighting; $\Delta k = 2.8$–11.3 Å^{-1}) of the data followed by inverse transformation over the range $\Delta r = 3.1$–5.2 Å (Figure 12A). The Fourier transform of this isolated EXAFS function is shown in Figure 12B,C. The high quality of these data (also see Figure 5C,D) suggests the worthiness of the challenge of the detailed analysis.

Since the number of adjustable parameters that can be estimated reliably from the data is only 12, a more than three-shell fit is not statistically justified. Therefore estimates were made by a combination of modeling and analysis of the data. Typically, the contribution for the smallest value of R was calculated with N and R according to the assumed model, with $\Delta\sigma^2$ and E_0 determined to give the best agreement with the data in r space. In the calculations, N^* ($N^* = N\exp[-2(R_r - R_{ref})/\lambda]$, with $\lambda = 6$ Å) was used to account for the difference in coordination distance between the reference compound and the contribution to be an-

TABLE III: EXAFS Results Characterizing the Sample Formed from Adsorption of $[H_3Re_3(CO)_{12}]$ on MgO, following Decomposition

shell	N^*	N^a	R, Å	ΔR,[c] Å	$\Delta\sigma^2$, Å^2	ΔE_0, eV	EXAFS ref
Re–C	3	3	1.883		0.0054	2	Os–C
Re–O*	3	3	3.091		0.0039	2	Os–O*
Re–O_{sup}	2.7	3	2.154	0	0.0055	−8	Re–O
Re–Mg_{sup}	3.7	4	2.797	−0.215	0.0139	1	Ir–Al
Re–O	2.2	4	3.635	−0.038	0.0098	−1.5	Re–O
Re–Re	0.9	1.33	3.940	−0.272	0.0006	4	Re–Re
Re–Mg[b]	0.6	1	4.335	0.075	0.0020	−10	Ir–Al
Re–O	3.1	8	4.690	−0.052	0.0172	−8	Re–O
Re–Mg	5	12	5.200	0.015	0.0160	7	Ir–Al

[a] Coordination numbers N are chosen according to the $Re(CO)_3[OMg]_3$ model. EXAFS analysis was done with coordination numbers $N^* = N\exp[-2(R - R_{ref})/\lambda]$ with $\lambda = 6$ Å. [b] Re–Mg: multiple scattering contribution. [c] ΔR is the difference between the coordination distance obtained from the EXAFS data analysis and the coordination distance calculated from a surface model in which it is assumed that the Re atoms lie directly above an oxygen atom in the MgO(100) face. The first Re–O coordination distance obtained from EXAFS (2.154 Å) is used to calculate the coordination distances in this model. The deviations in coordination distance observed in the first Re–$Mg_{support}$ and Re–Re shells indicate that the Re atoms do not lie exactly on top of the surface oxygen atoms but instead are slightly closer to each other.

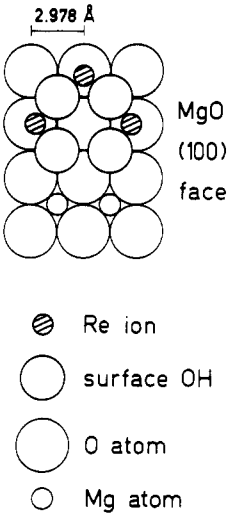

Figure 13. Structural model of a trirhenium ensemble formed by oxidative fragmentation of $[H_2Re_3(CO)_{12}]^-$ supported on MgO. The carbonyl ligands on Re are omitted for clarity. The structure was determined from EXAFS data.

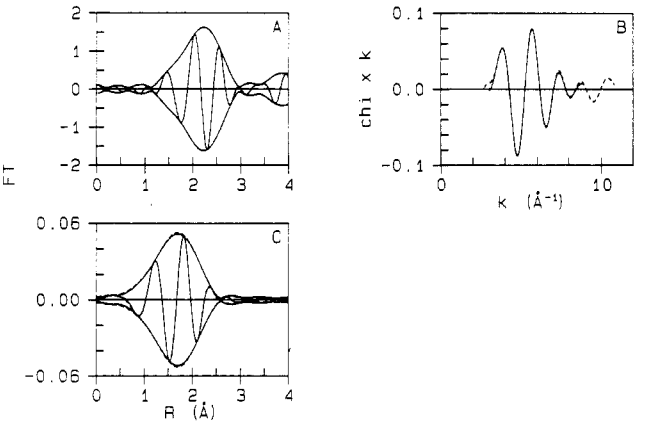

Figure 14. Results of EXAFS analysis characterizing the supported Re sample after treatment in H_2 at 350 °C: (A) raw EXAFS data, k^3 weighted, Δk = 3–9 Å^{-1}, Re–O phase corrected; (B) k^1-weighted isolated EXAFS (solid line) with three-shell fit (dashed line) in k space; (C) imaginary part and magnitude of normal Fourier transform (k^1 weighted, Δk = 3.5–8.5 Å^{-1}) of isolated EXAFS (solid line) and calculated Re–O contribution (dashed line; see Table VI).

alyzed. After this first-approximation contribution was subtracted, the next was treated in the same way. It was found that a Re–Re contribution at 3.94 Å was essential to give an acceptable agreement in r and in k space between the isolated higher shell data and the calculated EXAFS. Subsequently, all contributions were refined by subtracting all shells but the one to be improved from the data and then calculating a new one to agree as closely as possible with the difference file, now with only the value of N according to the model. The coordination parameters thus obtained for the discernible contributions are summarized in Table III. The EXAFS function incorporating all the contributions is shown in Figure 12A. The good agreement in r space between the data and the sum of the contributions is demonstrated in Figure 12B,C. The structural model agreeing best with the experimental EXAFS is depicted in Figure 13.

d. Reduction of the Surface Species Formed from the Fragmented Cluster. i. Treatment in Hydrogen at 350 °C. The quality of the data does not allow use of a Fourier transform range at values of $k > 9$ Å^{-1}. The imaginary part of the Re–O phase-corrected Fourier transform shows a positive peak at about 2 Å (Figure 14A). The asymmetry of the imaginary part points to the presence of another scatterer at about 2.5 Å.

Use of a Re–Re phase-corrected Fourier transform over an extended range of k (up to k = 12 Å^{-1}) did not show any peak corresponding to a metallic Re–Re distance. The quality of the EXAFS data in the range between k = 9 and 12 Å^{-1} is not sufficient to allow a conclusion. However, the XPS data collected with this sample indicate almost exclusively the presence of ionic and not metallic Re.[45] For further analysis, an EXAFS was isolated by using an inverse Fourier transform range Δr = 0–2.5 Å (Figure 5F). A two-shell fit (k^1 weighted) of this isolated EXAFS function resulted in the coordination parameters summarized in Table IV. The oxidation state (+4) of the Re ion makes the high value for the inner potential correction (12 eV; obtained with a Re^{6+} reference) of the Re–O coordination at 1.94 Å unlikely. Although the allowed number of adjustable parameters is only 9.5, we have done a three-shell fit (k^1) holding the Re–O distance of 2.54 Å fixed. Although this fit involves about two more adjustable parameters than are justified statistically and is therefore of questionable validity, we have included the results because they give more reasonable values for ΔE_0 with a much

TABLE IV: EXAFS Results Characterizing the Supported Re Sample after Treatment in H_2 at 350 °C

shell	N	R, Å	$\Delta\sigma^2$, Å^2	ΔE_0, eV	EXAFS ref	variance
Re–O	1.5	1.94	0.0027	12.4	Re–O	1.2×10^{-6}
Re–O	1.6	2.45	−0.0021	7.5	Re–O	
Re–O	0.8	1.90	−0.007	4.7	Re–O	
Re–O	1.9	2.10	−0.002	3.2	Re–O	1.3×10^{-7}
Re–O	3.3	2.45	0.007	6.7	Re–O	

(45) The XP spectrum of surface species formed by reducing $[H_2Re_3(CO)_{12}]^-[MgO]$ in H_2 at 350 °C for 4 h contained one broad peak (6.5 eV) centered at 43.6 eV. Re, ReO_2, and NH_4ReO_4 standards gave Re $4f_{7/2}$ peaks at 40.5, 43.3, and 46.5 eV, respectively. All binding energies were referenced to C 1s at 285.0 eV. These results suggest that a mixture of oxidized Re species was present on the MgO surface and that the predominant Re species had an oxidation state of +4.

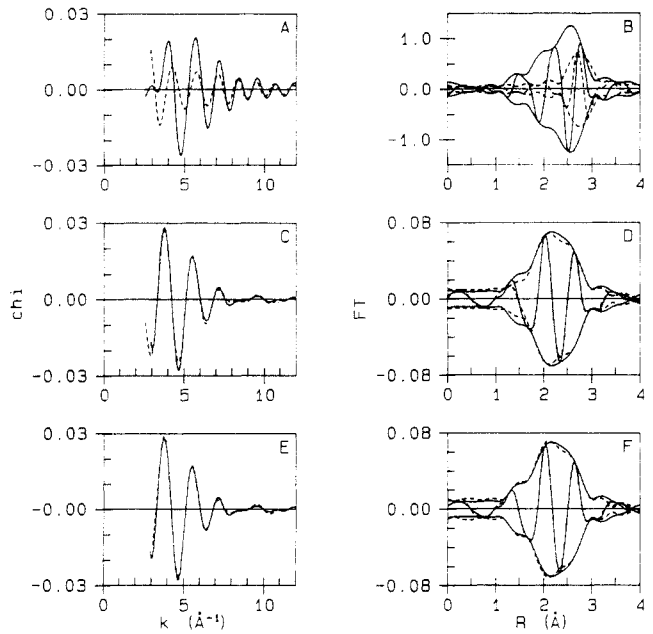

Figure 15. Illustration of the subsequent steps used in the difference file technique for analysis of the EXAFS data characterizing the supported Re sample after treatment in H_2 at 500 °C. (A) isolated first-shell EXAFS (solid line) and calculated Re–Re contribution (dashed line; see Table VII); (B) Fourier transform (k^1 weighted, Δk = 3.5–10.5 Å^{-1}, Re–Re phase and amplitude corrected) of spectra presented in A; (C) isolated first-shell EXAFS minus calculated Re–Re EXAFS (solid line) and calculated Re–O(s) (2.06 Å) + Re–O(l) (2.60 Å) EXAFS (dashed line); (D) Fourier transform (k^1 weighted, Δk = 3.5–10.5 Å^{-1}, Re–O phase corrected) of spectra presented in C; (E) isolated first-shell EXAFS minus calculated Re–Re EXAFS (solid line) and calculated Re–O(s) (2.06 Å) + Re–O(l) (2.60 Å) + Re–Mg (1.70 Å) (dashed line); (F) Fourier transform (k^1 weighted, Δk = 3.5–10.5 Å^{-1}, Re–O phase corrected) of spectrum presented in E.

better variance of the fit (Table IV). The fit (k^1) with three shells is displayed in Figure 14B. The agreement in r space between the Fourier transform of the data and the EXAFS function calculated with the coordination parameters (three shells) is shown in Figure 14C. The quality of the EXAFS spectrum with the short range of reliable data does not permit a clear choice between the two-shell and the three-shell fit.

ii. Reduction at 500 °C. A comparison of curves G and E of Figure 5 shows that, after treatment of the sample in H_2 at 500 °C, there were EXAFS oscillations evident at values of k up to 17 Å^{-1}. This result implies that ionic Re species were converted into Re crystallites as a result of reduction at the higher temperatures. To analyze the first-shell region of the Fourier transform shown in Figure 5H, an inverse Fourier transform was applied from r = 1.2 to 3.2 Å, resulting in an isolated first-shell EXAFS function (Figure 15A). To investigate the possible presence of scatterers in addition to those indicated by the main Re–Re contribution, a Re–Re phase- and amplitude-corrected Fourier transform was calculated with a k^1 weighting (making the Fourier transform sensitive to low-Z scatterers). The use of a k^1-weighted Fourier transform corrected for phase and backscattering amplitude of the metal–metal contribution to detect the presence of low-Z scatterers typified by the oxygen of the support has been discussed in papers dealing with the metal–support interface in supported metal catalysts.[33,37] The Fourier transform (Figure 15B) is asymmetric (both in its magnitude and its imaginary part) at the low-r side of the Re–Re peak located near 2.75 Å. This result indicates the presence of additional scatterers, since a proper phase and amplitude correction for the Re–Re contribution should result in a symmetric Fourier transform if no other contributions are present.

To analyze the EXAFS data further, the difference file technique was used together with fitting of the data in k space. First, the coordination parameters of the Re–Re contribution (being the largest component in the EXAFS spectrum) were determined from a fit in k space using only the high-k data. A Re–Re EXAFS function calculated with the first-guess parameters was then subtracted from the isolated first-shell EXAFS function. The data quality is high enough to permit further analysis of the difference file (Figure 15C). Two different contributions (Re–O at 2.60 Å and Re–O at 2.06 Å) are evident in the Re–O phase-corrected Fourier transform of the difference file (Figure 15D). First-guess parameters for these contributions were obtained by fitting the difference file in k space. The first-guess contributions were then added and compared with the first-shell isolated EXAFS data in k and in r space. To obtain a good fit in k and in r space, it was necessary to include a Re–Mg contribution at about 1.7 Å (Figure 15E,F). The agreement between the experimental results and the sum of the calculated contributions improved in subsequent fitting. A combination of a total fit in k space with simultaneous determination of each separate contribution in r space using the difference file technique resulted in the coordination parameters summarized in Table V. The good agreement in k and in r space between the isolated first-shell EXAFS and the sum of the individual contributions is demonstrated in Figure 16; 16 parameters were estimated, and the statistically justified number was 15 (Δk = 11.5 Å^{-1}; Δr = 2 Å).

7. Summary and Evaluation of Structural Characterizations. One of the primary goals of this research was to do precise synthesis on the MgO surface to produce ensembles of three Re complexes from $[H_3Re_3(CO)_{12}]$ and to characterize the surface structures with EXAFS spectroscopy and complementary techniques. The first step in the synthesis was intended to anchor the cluster—intact—to the support as a result of deprotonation of the cluster to form the surface-bound anion $[H_2Re_3(CO)_{12}]^-$. This chemistry was expected on the basis of the Brønsted acidity of the cluster in solution and is confirmed by characterization of the surface species by infrared and ultraviolet–visible spectroscopies and by the fact that the cluster anions can be extracted from the surface by cation metathesis and characterized in solution.

The EXAFS data confirm the formation of the cluster anion on the MgO surface. This conclusion follows from a comparison of the EXAFS spectrum of the initial surface species formed from $[H_3Re_3(CO)_{12}]$ with the spectrum of $[H_2Re_3(CO)_{12}]^-$ in the crystalline salt. Even a direct comparison of the Fourier transforms of the EXAFS data for these two samples shows the strong similarity of the Re species (Figure 17), and the structural parameters summarized in Table VI provide a strong confirmation. The

TABLE V: EXAFS Results Characterizing the Supported Re Sample after Reduction in H_2 at 500 °C

shell[a]	N	R, Å	$\Delta\sigma^2$, Å^2	ΔE_0, eV	EXAFS ref
Re–Re	6.3	2.74	0.0050	−4.8	Re–Re
Re–O(l)	1.3	2.60	−0.0052	3.1	Re–O
Re–O(s)	1.6	2.06	−0.0013	−4.5	Re–O
Re–Mg	0.3	1.70	−0.003	10	Ir–Al

[a] The l refers to long, and the s to short.

TABLE VI: Structural Comparison of $[H_2Re_3(CO)_{12}]^-$ in a Crystalline Salt and Adsorbed on MgO; Data Determined by EXAFS

	$[H_2Re_3(CO)_{12}]^-$[42]			$[H_2Re_3(CO)_{12}]^-$/MgO		
shell	N	R, Å	$\Delta\sigma^2$, Å^2	N	R, Å	$\Delta\sigma^2$, Å^2
Re–Re	2	3.246	0.0038	2	3.455	0.0010
Re–C	4	1.934	0.0024	4	1.912	0.0031
Re–O*	4	3.112	0.0018	4	3.089	0.0030

TABLE VII: Comparison of Re–C and C–O* Bond Distances in $[H_xRe_3(CO)_{12}]^{x-3}$ (x = 1–3) and in the Supported Cluster $[H_2Re_3(CO)_{12}]^-$/MgO

	bond dist, Å		
cluster	Re–C	C–O*	ref
$[H_3Re_3(CO)_{12}]$	1.976	1.126	42
$[H_2Re_3(CO)_{12}]^-$	1.934	1.178	42
$[H_2Re_3(CO)_{12}]^-$/MgO	1.912	1.177	this work
$[HRe_3(CO)_{12}]^{2-}$	1.83	1.24	43

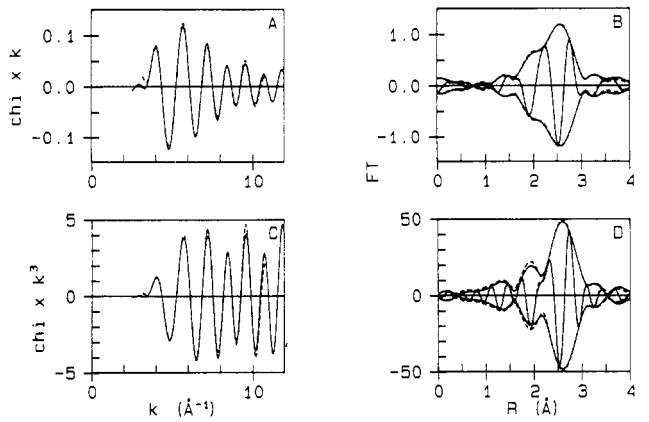

Figure 16. Results of the final EXAFS analysis for the supported Re sample after treatment in H_2 at 500 °C: (A) isolated first-shell EXAFS (k^1 weighted, solid line, and best k^1-weighted, fit, dashed line); (B) Fourier transforms (k^1 weighted, Δk = 3.5–10.5 Å^{-1}, Re–Re phase and amplitude corrected) of spectra presented in A; (C) isolated first-shell EXAFS (k^3 weighted, solid line) and best k^3-weighted fit (dashed line); (D) Fourier transforms (k^3 weighted, Δk = 3.5–10.5 Å^{-1}, Re–Re phase and amplitude corrected) of spectra presented in C.

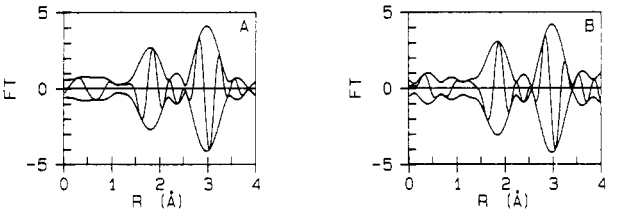

Figure 17. Comparison of the EXAFS results for (A) the sample prepared by adsorption of $[H_3Re_3(CO)_{12}]$ on MgO and (B) $[(C_6H_5)_4As][H_3Re_3(CO)_{12}]$ (k^3 weighted, Δk = 3.6–10.2 Å^{-1}, Re–O phase corrected).

results of an EXAFS characterization[42] of the molecular clusters $[H_xRe_3(CO)_{12}]^{x-3}$ (x = 2, 3) are summarized in Table VII with the results obtained in this work for the supported cluster anion. The C–O* bond length in $[H_2Re_3(CO)_{12}]^-$ is the same as that of the supported analogue, and the Re–C bond lengths are also nearly the same in the supported and molecular clusters. These results provide a strong confirmation of the conclusion that $[H_3Re_3(CO)_{12}]$ is deprotonated upon adsorption on MgO.

The differences in the coordination parameters shown in Table VI provide further insight into the surface chemistry. The average Re–Re distance is 0.2 Å greater in the supported cluster than in the analogous molecular cluster. This result suggests a distortion of the triangular metal framework on the support surface, and the suggestion is supported by the result that the Debye–Waller factor for the Re–Re contribution characterizing the supported cluster is distinctly larger than that characterizing the molecular cluster. The EXAFS results show the presence of one Mg neighbor for every two Re atoms anchored to the surface. No indications of a direct interaction between these Re atoms and support oxygen are evident in the EXAFS results.

Heating the supported cluster anion leads to fragmentation of the metal framework and oxidation of the Re; this conclusion has been demonstrated by infrared, Raman, and inelastic electron tunneling spectra of the resulting supported Re complexes.[30] The complexes have been formulated as $[Re(CO)_3\{HO\text{-}Mg\}_2\{O\text{-}Mg\}]$.[30] The symmetry indicated by the infrared spectra showed that there were two different kinds of surface ligands (noncarbonyl ligands),[30] but the identification as oxygen ions and hydroxyl groups still remains uncertain. The EXAFS data are consistent with the structural inferences.

The Debye–Waller factors characterizing the Re–C and the Re–O* bonds in the supported mononuclear Re complex (Table III) are greater than those characterizing the supported cluster anion, pointing to a greater disorder in the Re—C≡O bonds. The difference in disorder between the Re–C and Re–O* coordinations can be interpreted as evidence that the Re–C–O bond angle is closer to 180° in the mononuclear Re complex than in $[H_3Re_3(CO)_{12}]$.[41,42]

A striking result is the indication in the EXAFS data of neighboring Re centers in the surface structure formed by breakup of the supported trirhenium clusters, at an average distance of 3.94 Å. The significance of this result is that it provides evidence that the desired ensembles were formed on the MgO surface; evidently, the Re atoms remained near each other on the support as the cluster anion was fragmented, with the resulting Re ions becoming bonded directly to oxygen ions of the support surface. This Re–Re distance is distinctly different from the Re–Re distance in bulk Re metal (2.75 Å), and the data are consistent with the inference that no metallic Re was formed during the decomposition of the cluster anions.

In the model of the ensemble consisting of three Re carbonyl complexes on the MgO surface (Figure 13), the distances (Table III) are shown to scale. It is assumed that the structure exists on the MgO(100) surface (the predominant surface of MgO), and the distances shown for MgO are the crystallographic values for the bulk solid. In the model calculations, it was assumed that each Re atom lies directly above an oxygen atom in the MgO(100) face. The differences between the coordination distances derived from the EXAFS results and the surface model are shown in the fifth column of Table III. The two other oxygen neighbors detected with EXAFS might be in hydroxyl groups present in positions slightly different from those of the surface oxygen ions. The Re–O distance (2.154 Å) derived from EXAFS was used to calculate the coordination distances in the model. The deviations in coordination distance observed in the first Re–Mg and Re–Re shells provide evidence that the Re atoms do not lie exactly on top of the surface oxygen atoms as is shown in Figure 13. This geometry may be the result of a distortion induced by the surface hydroxyl groups. We emphasize that this is a simplified model; it is consistent with the EXAFS data, but other arrangements of the Re atoms on the surface are possible. The important point is that there are near-neighbor Re atoms.

When the supported Re sample formed by oxidative fragmentation of the supported trirhenium cluster was treated in H_2 at 350 °C, it was found to be catalytically inactive for cyclopropane hydrogenolysis. This result suggests that the Re had been oxidized by this treatment. Consistent with this interpretation, no evidence for Re metal in this sample was found with EXAFS. The suggestion of oxidized Re is supported by the results obtained with XPS, which show a binding energy indicative of an average Re oxidation state of +4.[45]

The EXAFS results show two Re–O coordination shells, at 1.94 and 2.45 Å. The Re–O coordination distance of 1.94 Å is in reasonable agreement with that found in ReO_2. The Debye–Waller factor obtained for this shell suggests a large degree of disorder. The coordination number (between two and three) indicates that the Re ions take the same position on the surface as the $Re(CO)_3$ entities, on top of a MgO oxygen atom and coordinated to two (or one) surface hydroxyl groups (Figure 13). When this situation was simulated in a three-shell fit, indeed it was found that the Re–O contribution at 1.97 Å can also be attributed to a sum of two Re–O shells: one with N = 0.8, R = 1.90 Å, $\Delta\sigma^2$ = −0.007 Å^2 (MgO oxygen), and another with N = 1.9, R = 2.10 Å, $\Delta\sigma^2$ = −0.002 Å^2 (surface hydroxyl groups). Although the range of EXAFS data is evidently too short to allow an accurate three-shell fit, it is apparent that the coordination of the Re ion to MgO oxygen and surface hydroxyl groups, with different coordination distances, is well possible.

The other EXAFS Re–O shell, with a coordination distance of 2.45 Å, is very likely indicative of other oxygen-containing ligands such as hydroxyl groups, which have replaced the CO ligands of the $Re(CO)_3$ entities during decomposition. EXAFS results show that three or four of these ligands are present. Also for this shell, large disorder is found, and thus it is possible that the ligands are present at different Re–O distances.

No sign of a Re–Mg coordination at approximately 2.85 Å was found, although this was expected on the basis of the proposed

surface structure (similar to that of Figure 13). An attempt was made to include a Re–Mg contribution in the analysis. The short range of useful EXAFS data, however, prevented our deciding unambiguously whether the Re–Mg contribution is present.

The EXAFS data characterizing the surface species formed by heating the sample formed from $[H_3Re_3(CO)_{12}]$ on MgO to 500 °C in H_2 for 1 h clearly demonstrate the presence of Re crystallites. This conclusion is consistent with the catalysis results presented elsewhere,[46] which demonstrate that the supported crystallites have catalytic properties similar to those reported for Re metal powder.

Besides the Re–Re coordination at 2.74 Å, significant contributions of three other shells were obtained (Table V). On the basis of EXAFS results for Rh/MgO and Ir/MgO,[40] we suggest the Re–O(l) (l refers to long) and Re–Mg shells are associated with the metal–support interface. The Re–O(s) (s refers to short) contribution at 2.06 Å is difficult to associate with the metallic Re particles.

We suggest that the Re–O(s) contribution is evidence of a remnant of the oxidized Re entities proposed for the sample after reduction at 350 °C. This means, judging from the coordination number obtained, that at least 30% of the Re in the sample was not yet reduced. (In the EXAFS technique, overall coordination numbers are obtained. If two or more different phases containing Re coexist, the coordination numbers are to be corrected for the fraction of Re present in each phase, in order to yield the true coordination numbers.[37])

Correction for an unreduced fraction of 30% yields the following coordination numbers for the reduced phase: N(Re–Re) = 9.1 and N[Re–O(l)] = 2.3. From the Re–Re coordination number it follows that the average diameter of the metallic Re particles is approximately 25 Å, assuming that these particles are hemispherical. The Re–Re and Re–O(l) coordination numbers are in agreement with a Re–MgO interface model in which the interface Re atoms are 4-fold coordinated by oxygen.[37,40] As MgO exhibits predominantly (100) faces, it is most probable that the interface is (100)-like and that the Re atoms are positioned directly on top of the surface Mg atoms in the (100) face of MgO. In view of the rather small Debye–Waller factor found for the Re–O(l) shell (indicating a well-ordered interface), it is most probable that the Re crystallites are also bounded by a (100) face in the metal–support interface. This kind of epitaxy has already been suggested for Rh/MgO and Ir/MgO structures.[40] Thus we suggest that a gradual change will take place in the Re crystallites from fcc [the (100) face] in the Re–MgO interface to hcp in the bulk of the metal crystallites. This suggestion is supported by the rather large Debye–Waller factor for the Re–Re contribution, which suggests the structural disorder in the Re–Re shell that should accompany such a transition.

(46) Kirlin, P. S.; Knözinger, H.; Gates, B. C. *J. Phys. Chem.*, following paper in this issue.

Conclusions

The initial interactions of $[HRe(CO)_5]$ and of $[H_3Re_3(CO)_{12}]$ with the basic MgO surface closely parallel the chemistry of these and analogous complexes in basic solution. The nature of the chemisorption of the Re complexes on MgO is related to their solution pK_a's, which are 3.5 and 21.4 for $[H_3Re_3(CO)_{12}]$ and $[HRe(CO)_5]$, respectively. The precursor $[H_3Re_3(CO)_{12}]$ is completely ionized by the MgO, whereas $[HRe(CO)_5]$ is not completely deprotonated by the basic surface.

The surface complexes react in He or H_2 or under vacuum upon heating to 80 °C (in the case of $\{MgO\}H^+\cdots[Re(CO)_5]^-$) or to 225 °C (in the case of $[H_2Re_3(CO)_{12}]^-\{MgO\}$) to give a rhenium subcarbonyl suggested to be $[Re(CO)_3\{OMg\}\{HOMg\}_2]$. The reaction of the trinuclear cluster begins with CO dissociation followed by the oxidative addition of surface hydroxo ligands. The surface chemistry is summarized in Scheme I. The difference in reactivity between the mononuclear complex and the cluster is attributed in part to the stability provided by the metal framework in the cluster.

An essential difference between the mononuclear complex and the cluster is that $[HRe(CO)_5]$ gives possibly isolated Re subcarbonyls, whereas $[H_3Re_3(CO)_{12}]$ gives trinuclear ensembles of the same Re subcarbonyls. The average distance between the Re atoms in the latter units in the ensemble is 3.94 Å. Upon treatment of this sample in H_2 at 500 °C, Re metal particles are formed on the support, but the reduction is not complete, with some uncharacterized Re species being present with the metal particles.

The several materials are markedly different in catalytic performance, as summarized in a companion paper.[46]

Acknowledgment. We thank K. M. Sanchez of the University of Delaware for helpful discussions. Most of the EXAFS experiments were carried out at Cornell University at the Cornell High Energy Synchrotron Source (CHESS). Additional EXAFS experiments were carried out on beamline X-11A at the National Synchrotron Light Source (NSLS) at Brookhaven National Laboratory and at the Stanford Synchrotron Radiation Laboratory (SSRL). We are grateful to the synchrotron staffs for their assistance. This work was supported by grants from the donors of the Petroleum Research Fund, administered by the American Chemical Society, the U.S. Department of Energy, Office of Energy Research, Office of Basic Energy Sciences (FG02-87ER13790), and the Exxon Education Foundation.